3-8 Mobile Whole-head SQUID System of SNS Junctions in a Superconducting Magnetic Shield

OHTA Hiroshi and MATSUI Toshiaki

We have constructed a mobile whole-head SQUID system of SNS (Superconductor/Normal metal/Superconductor) junctions in a superconducting magnetic shield. The whole-head SQUID system in the superconducting magnetic shield is 100 times more sensitive than that in a magnetically shielded room of Permalloy. Nanometer-scale SNS junctions have the comparable size to the wavelength of the beat of de Bloglie waves of an electron and a hole to be a mesoscopic system. The established theory of mesoscopic SNS junctions is as elegant as Planck theory of blackbody radiation. SQUID systems enable invasive studies about recognition in human brains. They have response time of millisecond to be a good tool for experimental confirmation of neural models of human brain obtaining information about memory, attention and learning in long latencies. They are expected to make some contribution to studies about autism, ADHD and LD.

The SQUID system has successfully detected magnetic fields from human brains both in crowded Nano tech 2003 held at Makuhari Messe convention center and Nanotech 2004 at Tokyo Big Sight Exhibition Center. The success could be the first step to mobile clinic for mental care.

Keywords

Mobile, SQUID, Mesoscopic josephson junction, Superconducting magnetic shield, Tonic and burst mode, Thalamo-cortical network

1 Introduction

The mobile SQUID system in Fig.1 has been made of both of a superconducting magnetic shield of high-Tc superconductor BSCCO and SQUIDs of low-noise SNS Josephson junction.

SQUID (Superconducting Quantum Interference Device) is a sensitive magnetometer using the interference of supercurrent to detect weak magnetic field from human brains to be the third generation CT scanner next to X-ray CT and MRI. Patients of SQUID-CT or MEG(MagnetoEncephaloGraphy) are not exposed to X-rays because MEG invasively detects weak magnetic fields generated by

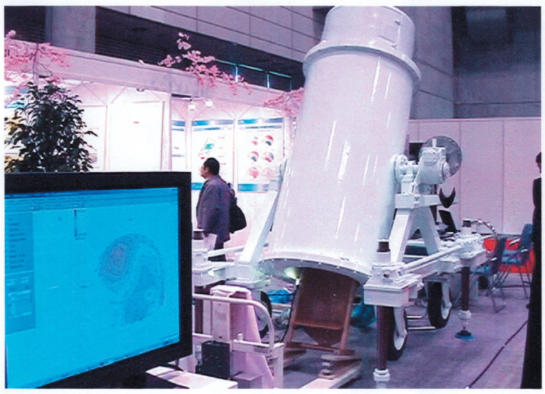

Fig.1 Mobile SQUID system in operation at Makuhari Messe convention center

current dipoles in brains. MRI invasively obtains anatomical information of brains while MEG invasively obtains information about functions and activities of brains. MEG can tell whether a brain is in a awake state or in sleep for instance. Functional-MRI displays distribution of hemoglobins with oxygen to measure physiological changes which are not as fast as neural changes of mllisecond measured easily by MEG. We gave successful demonstration of the mobile 64-channel SQUID system of SNS junction in the superconducting magnetic shield in Nanotech 2003 at Makuhari Messe convention center in February 26-28 , 2003 as shown in Fig.1 to win Nanotech 2003 Award. This successful demonstrtion could be the first step to realization of mobile clinic for mental care. The SQUID system required development of two technologies - a low noise SQUID of SNS junction and a large superconducting magnetic shield.

2 Magnetic shield of high Tc oxide superconductor

Magnetic field generated by nerve currents in brains are one hundred million times weaker than the earth magnetic field as shown in Fig.2.

Therefore some magnetic shields are essential to reduce fluctuations of the earth magnetic field. Magnetically shielded rooms of Permalloy - a high permeability nickel alloy are still being used in conventional SQUID sytems to reduce magnetic noises in sorroundings while we have developed a diamagnetic superconducting magnetic shield of high-Tc superconductor [1]-[4]. Ambient magnetic noises are more than ten times larger in peak traffic than in light traffic around 0.1 Hz in Fig. 3 [6]. Most ambient noises in downtown are generated mostly by automobiles and subways moving around inside a circle of several killometer radius to have a peak below 1 Hz. Therefore magnetic shields for SQUID systems must shield magnetic noises below 1 Hz as well as above 1 Hz. The experimental data in Fig.3 indicates that the shielding factor of the superconducting shield does not degrade even below 1 Hz while the shielding factor of

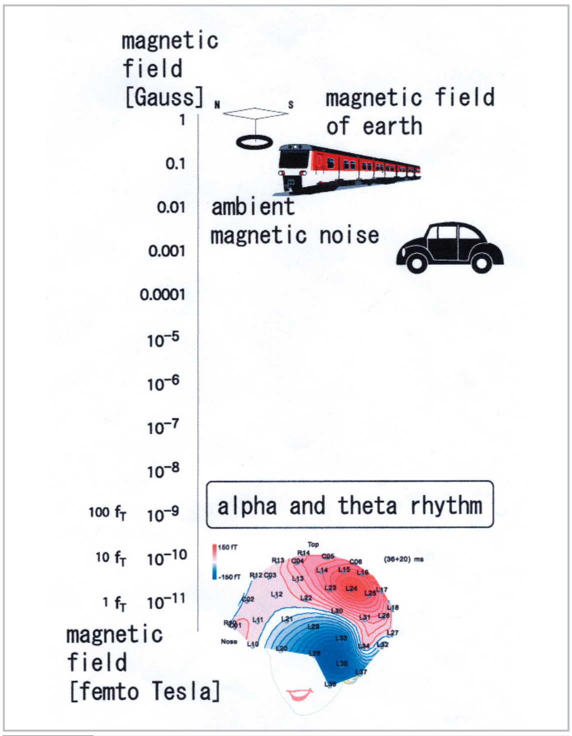

Fig.2 *Ambient magnetic noise versus brain magnetic field*

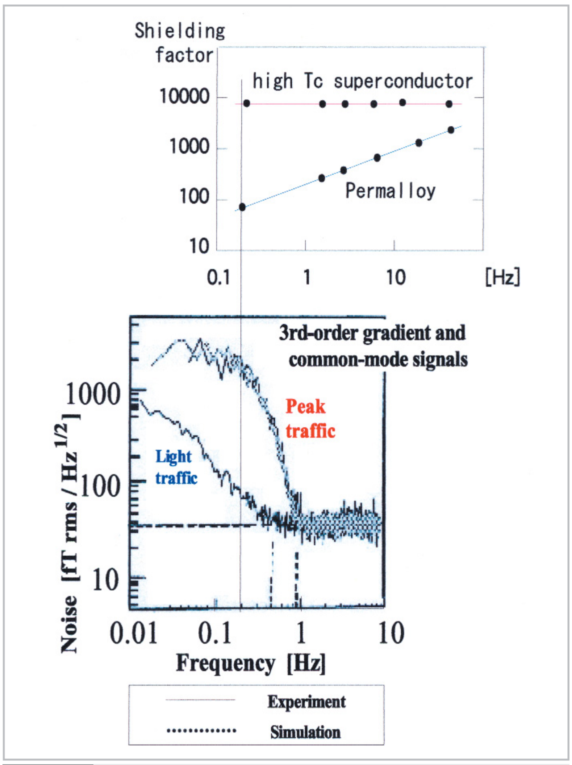

Fig.3 *Frequency dependence of high Tc supercondutor and Permalloy. Most ambient magnetic noises are located below 1 Hz.*

the shield of ferromagnetic Permalloy degrades below 1 Hz as shown in Fig.3. The shielding factor is the ratio of the magnetic field outside a shield to that inside the shield. The superconducting shield uses Meissner effect of perfect diamagnetism which is different from high permeability of Permalloy by nature.

We started with measureing shielding factors of high-Tc superconductors by means of induction method fortunately rather than a DC method such as the Hall effect to recognize the merit of high-Tc superconductors - shielding factor of three million at 0.2 Hz for the first time in the world. The superconducting magnetic field is made of high Tc phase of lead-treated $Bi_xPb_{(2-x)}Sr_2Ca_2Cu_3O_y$. It is a cylinder of 65 cm in diameter and 160cm in length to shield human bodies including head from magnetic noises as shown in Fig.7. Silver and then 1mm thick $Bi_xPb_{(2-x)}Sr_2Ca_2Cu_3O_y$ are plasma-splayed onto the inside wall of the cylinder of 65 cm in diameter and 160cm in length in the atomosphere. The silver layer prevents interdiffusion between the BSCCO film and the nickel cylinder during annealing of 830 degree Centigrade. The critical temperature of BSCCO is 103 K. The critical temperature of 103 K would not be obtained unless the temperature is kept to be 830 ± 5 degree centigrade everywhere of the nickel cylinder during a week of annealing. The cylinder of superconductor is free from mechanical vibrations during SQUID measurement because it is cooled down to cryogenic temperature by circulating helium gas sent from a closed-cycle helium refrigerator. Therefore all part of the superconducting magnetic shield tilted at any angles is kept below 77 K to be superconducting because the shield does not suffer from changes in level like liquid nitrogen. Noise spectra are measured by the same SQUID sensors inside the superconducting shield to be compared with those measured in a shielded room of Permalloy as shown in Fig.5. The sensitivities inside the superconducting shield are more than 100 times better than those in a shielded room of Permalloy below 1 Hz .

Fig.4 *The SQUID dewar is inserted horizontally.*

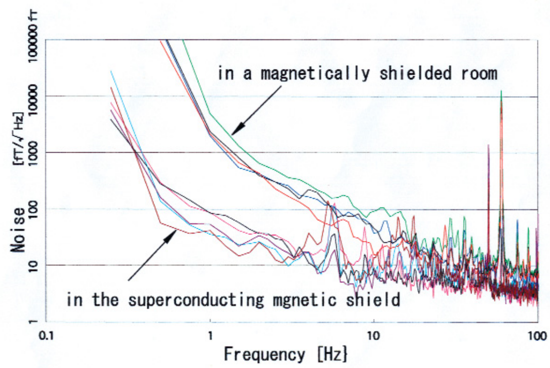

Fig.5 *The sensitivities inside the superconducting shield are more than 100 times better than in a shielded room of Permalloy below 1 Hz .*

The SQUID dewar of FRP is inserted or removed horizontally for maintenance without use of a chain block lift in the ceiling.

3 SNS junction as an electron-wave device

The SQUID magnetometors in the whole-head-type 64-channel SQUID system in the superconducting magnetic shield are made of SNS (superconductor/normal metal/superconductor) junctions.

An electron behaves as a wave instead of a particle in a region of comparable size to de Broglie wavelength λ=h/p where h is Planck constant. The de Broglie wavelength is shorter than 1 nm when the momentum $p=mv$ is close to that of electrons in a silicon device at room temperature. The de Broglie wavelength of an electron in a compound semionductor is about 10 nm because the effective mass of an electron there is several tens of times smaller than that of an electron in silicon devices. An electron beam lithography can make devices of 10nm size. The electron-beam lithography can realize a SNS junction as an electron-hole beat-wave device because the difference $p=p_e-p_h$ between the momenta of an electron and a hole carrying current in the N-region of a SNS junction makes a contribution to the de Broglie wavelength of 10 mn. In fact, the N-region of a SNS junction in Fig.9 is shorter than 10 nm, 10∼13 nm thick and 150 nm wide. A SNS junction is a mesoscopic system whose sizes are comparable to the wavelength of the beat between the de Broglie waves of an electron and that of a hole.

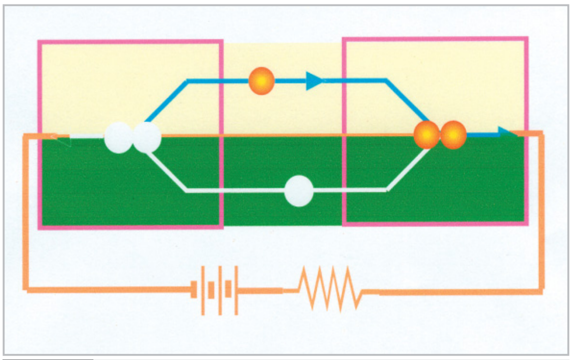

Fig.6 *Andreev reflection in a mesoscopic SNS junction*

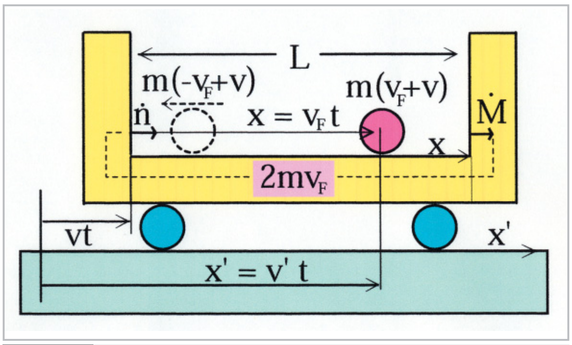

Fig.7 *The billiard model of a SNS junction*

The established theory of SNS junction is one of most elegant theories. A SNS junction in the ballistic (clean) limit is simulated by the billiard model in Fig.7. Gutzwiller trace formula gives a semiclassical Green function.

$$G_{semiclassical} = \frac{1}{i\hbar\nu}\sum_{n=0}^{\infty}\exp\left[-in\left(\frac{1}{\hbar}\oint pdx+\phi+\pi\right)\right]$$

Gutzwiller trace formula can express the quantum level density in terms of parameters of the correponding classical periodic motion yielding the semiclassical (Bohr-Sommerfeld) quantization condition for the trajectory in Fig.6.

$$\rho(E) = -\frac{1}{\pi}\mathrm{Im}G_{semiclassical} =$$

$$= \frac{1}{N}\sum_{n=-N}^{N}\delta\left[\left(\oint pdq+\hbar\phi\right)\nu-\left(n-\frac{1}{2}\right)2\pi\hbar\nu\right]$$

$$= \delta\left(E-\Delta\cos\frac{\phi}{2}\right)+\delta\left(E+\Delta\cos\frac{\phi}{2}\right)$$

The expectation value for any observables can be calculated by the density of states.

$$F = -k_BT\int_{-\infty}^{\infty}\ln\left(1+e^{-E/k_BT}\right)\rho(E)dE$$

$$= -k_BT\left\{\ln\left(1+e^{-\frac{\mathcal{E}}{k_BT}}\right)+\ln\left(1+e^{\frac{\mathcal{E}}{k_BT}}\right)\right\}$$

$$= -k_BT\sum_{\sigma=\uparrow,\downarrow}\ln\left(2\cosh\frac{\mathcal{E}}{2k_BT}\right)$$

$$S = -\left(\frac{\partial F}{\partial T}\right)_N =$$

$$= -k_B\sum_{\sigma=\uparrow,\downarrow}\{f\ln f+(1-f)\ln(1-f)\}$$

$$E = F+TS =$$

$$= \mathcal{E}f-\mathcal{E}(1-f) = \sum_{\sigma=\uparrow,\downarrow}\mathcal{E}\left(f-\frac{1}{2}\right)$$

where

$$\mathcal{E} = \Delta\cos\frac{\phi}{2}\ , \qquad f = \frac{1}{e^{\mathcal{E}/k_BT}+1}$$

All of the thermodynamic potentials are the sum of two terms coming from contribution of the electron-like quasi-particle state and the hole-like quasi-particle state.

The thermodynamic potentials of the Fermion oscillator are to be compared with those of the Boson oscillator or Planck theory of black-body radiation.

$$F = k_BT\sum_{\omega,\sigma}\ln\left(2\sinh\frac{\hbar\omega}{2k_BT}\right)$$

$$S = -k_B \sum_{\omega,\sigma} \{ f_\omega \ln f_\omega - (1+f_\omega) \ln (1+f_\omega) \}$$

$$E = \sum_{\omega,\sigma} \hbar\omega \left(f_\omega + \frac{1}{2} \right)$$

$$f_\omega = \frac{1}{e^{\hbar\omega/k_B T} - 1}$$

When we noticed of the beatiful symmetry reading a Planck text book of black body radiation, we decided to continue the calculation about the dirty-limit SNS juntion in terms of random matrix theory.
When the transmission coefficient T_p is not equal to zero more generally, the bound state energy ε of the electron-like quasipqrticle and the hole-like quasipqrticle in the N-region is given by

$$\mathcal{E} = \pm \Delta \sqrt{1 - T_p \sin^2 \frac{\phi}{2}}$$

The free energy gives the supercurrent penetrating the normal metal barrier.

$$I = \frac{2e}{\hbar} \frac{\partial F}{\partial \phi} = \frac{e\Delta}{2\hbar} \sum_{p=1}^{N} \frac{T_P \sin\phi}{\sqrt{1 - T_P \sin^2 \frac{\phi}{2}}} \times$$

$$\times \tanh \left(\frac{\Delta}{2k_B T} \sqrt{1 - T_P \sin^2 \frac{\phi}{2}} \right)$$

This general representation of Josephson current can explain all of three types of Josephsonn junctions in Fig.8 which used to be described by three independent theories. Namely only difference among three types of Josepson junctions is the difference in value of transmission coefficient T_p. The current has temperature dependence of a tunnel Josephson junction when the transmission coefficient is very close to zero. It has temperature dependence of a clean limit weak link when the transmission coefficient is very close to unity. The current has temperature dependence of a dirty limit weak link when the transmission coefficient has a statistical distribution between zero and unity. The situation is similar to Maxwell equations which unified radio wave, optical light and X-ray of differnt wavelengths.

Later on, the general theory has turned out to be only theory which can explain temperature dependence of Josephson currents of high Tc oxide superconductors. SQUIDs of clean-limit SNS junctions have the lowest noise

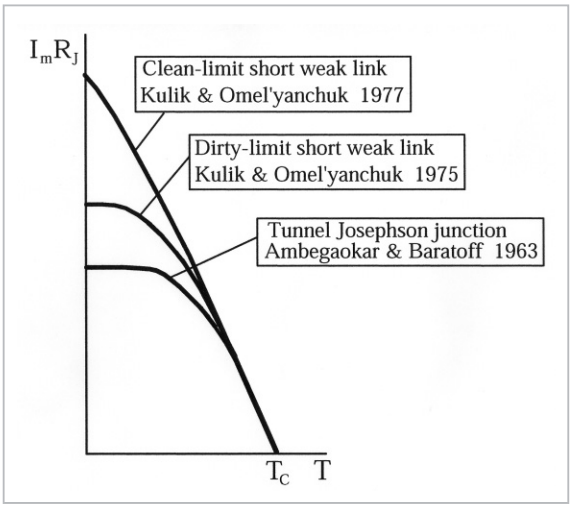

Fig.8 *Three different types of Josephson junctions*

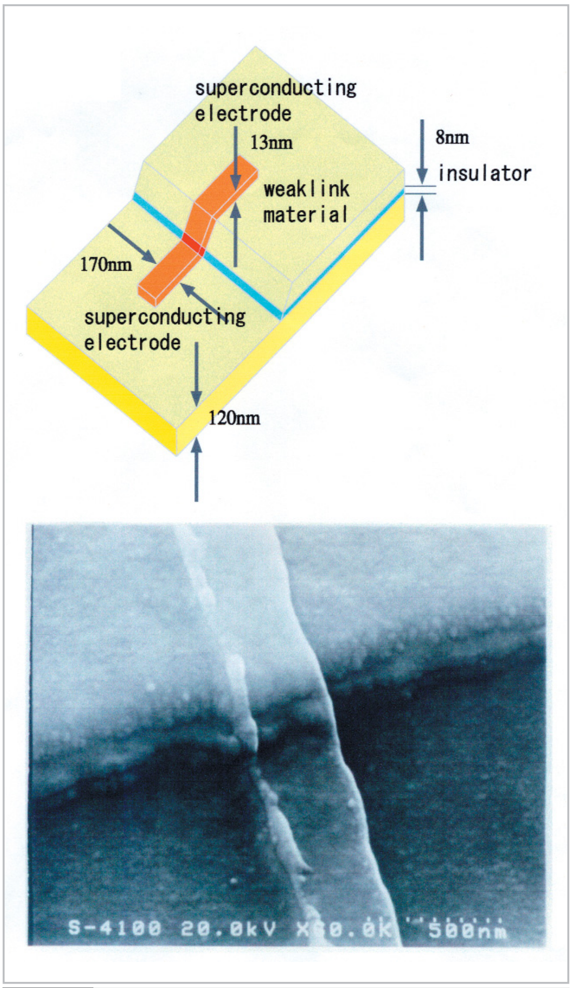

Fig.9 *Sizes of a fabricated SNS junction*

temperature among three types of Josephson junctions. SIS tunnel junctions have low-frequency telegraph-noise caused by randomly charged and discharged electrons on the insulator barrier like in MOS FET transistors.

4 Neuromagnetic SQUID measurements

We observed somatosensorily evoked signals as shown in Fig.10 stimulating the median nurve in the right list of patients by current

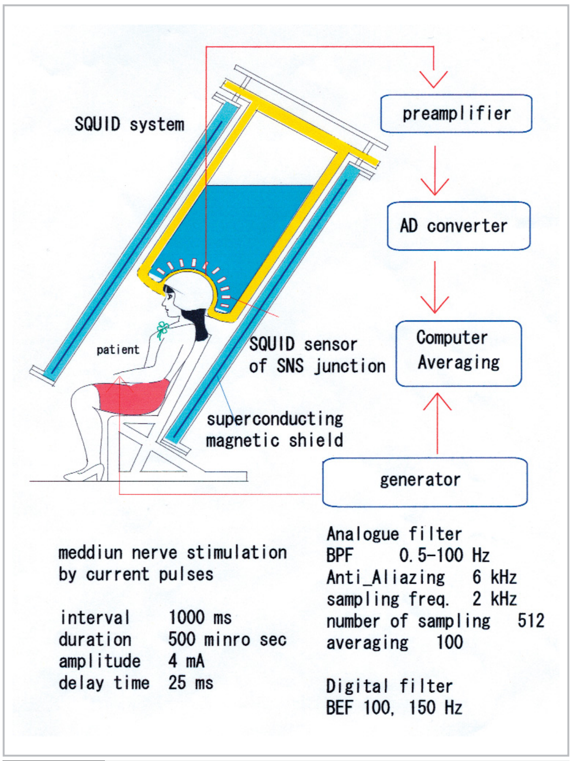

Fig.10 *Whole-head SQUID system*

pulses. Figures 11 through 13 show outputs from the 64-channel whole-head SQUID system which has a sensitivity of about 5 fT (10^{-15} Tesla)／$\mathrm{Hz}^{\frac{1}{2}}$. It means a sensitivity of 50 fT with a bandwidth of 100Hz. Therefore the averaging of 100 data gives a sensitivity of 5 fT. The evoked current dipole indicated by red arrows in Fig.12 is located at cetral sulcus of MRI data when the median nurve in the right wrist of the patient is stimulated by electrical current pulses. We can easily make sure that the magnetic fields above the skull are in a clockwis-screw direction of the red arrow at

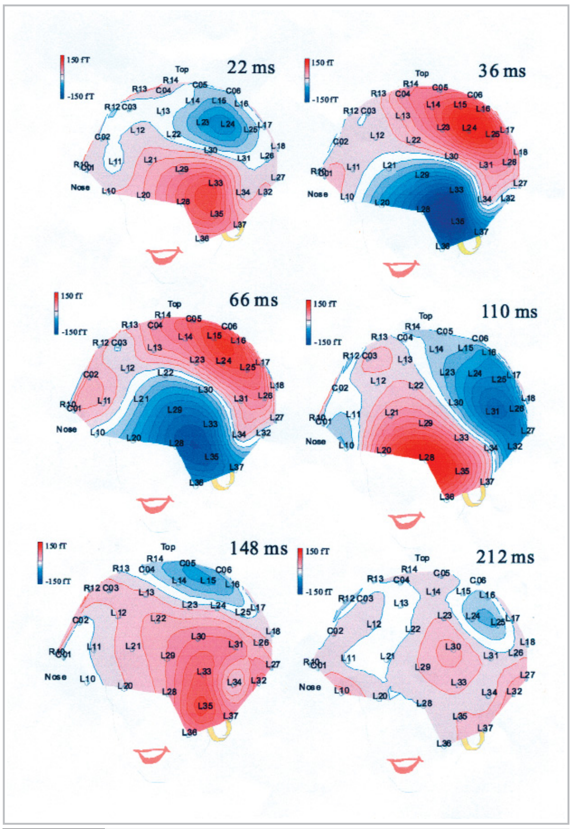

Fig.11 *somatosensorily evoked signals The direction of nurve current is reversed between 66ms and 110ms after the stimulation when the polarity of magnetic fields are also reversed.*

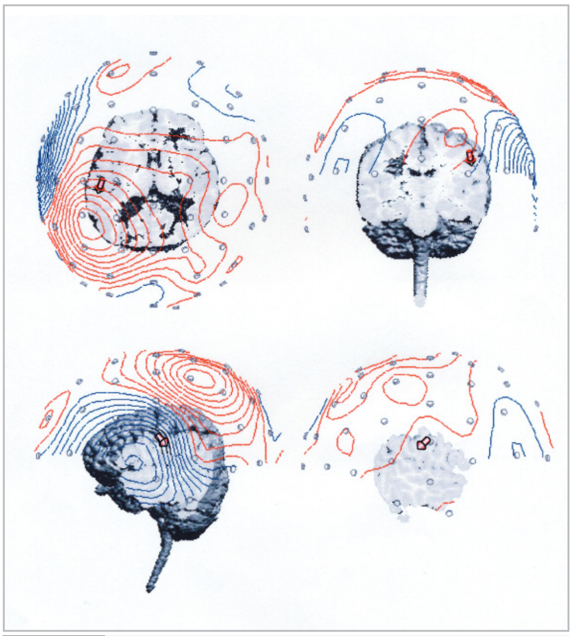

Fig.12 *Data of SQUID and MRI are superimposed to identyfy the location(cetral sulcus) of the evoked current dipole(red arrow) which is evoked by stimulation of the meiun nerve in the right wrist.*

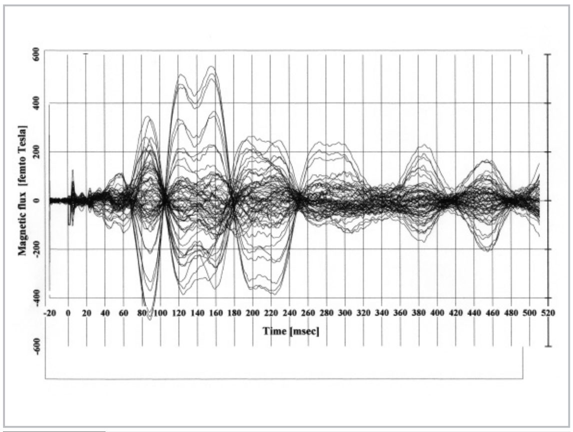

Fig.13 *Data of 64 channel whole-head SQUID system in the superconducting magnetic shield.*

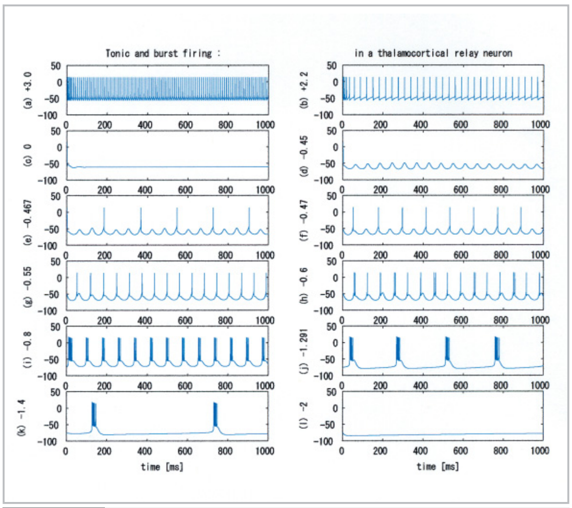

Fig.14 *Relay neurons in a thalamus work as a pacemaker depending on membrane potential.*

the two figures in left row of Fig.12.

Figure 13 shows 64 traces of each channel versus the common time axis. Theta rhythms are observed at longer latencies than 250 ms. The nodes of the theta rhythm are very narrow even at longer latencies than 250 ms just indicating a small low-frequency noises. Most sensory responses of human brains phase out within 250 ms. The current dipoles at the secondary somatosensory area SII is evoked at longer latecies than 250 ms making contribution to a higher function of brains than senses. These rhythmic after-discharges at long latencies are caused by after-depolarization or ahter-hyperpolarization at synapses.

Let us take a thalamus as an example to study more details of brain activities at long latencies. Almost all sensory inputs including visual, auditory or somatosensory stimulation are projected to the corresponding cortex through thalamus [10]. Relay neurons in a thalamus can generate rhythms alone to be as a pacemaker whose frequency depends on membrane potential as shown in Fig.14. The neural model of Wang about thalamus gives similar results to the standard model of Hindmarsh and Rose [8][9]. Thalamus generates rhythmic-(tonic-)mode rhythms ((a) and (b) in Fig.14) when the membrane potential is higher than the resting potential while it generates burst-mode rhythms ((e),(f),(g),(h),(i),(j),(k) in Fig.14) when the membrane potential is lower than the resting potential [7]. Thalamus does

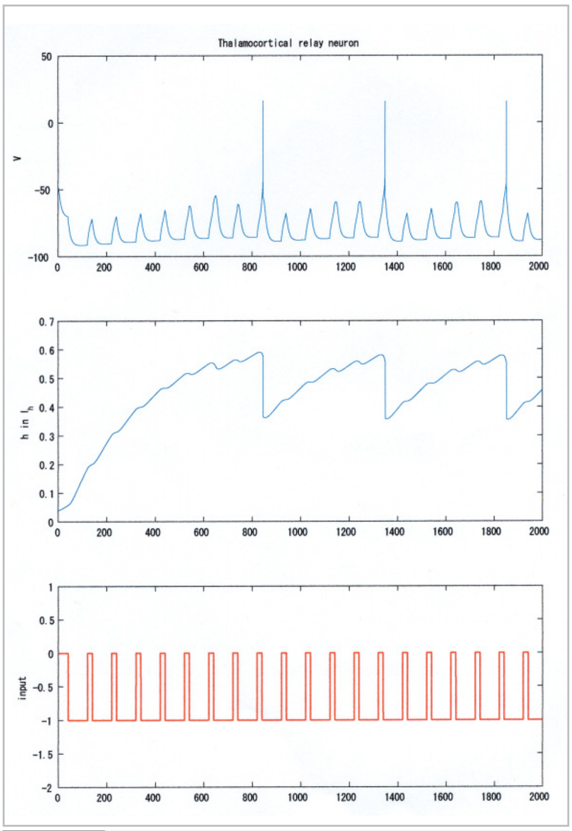

Fig.15 *Mechanism of one-fifth frequency division or adaptation in a relay neuron in a thalamus. The time constant is about 1000ms=1sec.*

not generate any rhythms when it is in a state (c) in Fig.14. However the thalamus in the state (c) starts to generate tonic mode rhythms when it receives excitatory inputs of ACh(acetylcholine) through locus ceruleus and basal nucleus of Meynert and it starts to generate burst mode rhythms when it receives inhibitory inputs of serotonin from the raphe nuclei. The frequency division of one third and one half are observed in (e) and (f) in Fig.14. The mechanism of frequency division in brains as shown in Fig.15 is similar to that of multivibrators in electronic circuits. The frequency division of one fifth is observed in the data in Fig.15. Choice among one third , one fifth or more is controlled by the bias voltage in an electronic circuit or the hyperpolarization-activated cation current I_h whose time constant is

$$\tau_h = \left\{\exp\left(\frac{V+66.4}{9.3}\right) + \exp\left(-\frac{V+81.6}{13}\right)\right\}^{-1}$$

to be 1 sec for $V =$ -74.5 mV . The inverse of 1 sec is 1Hz. Experimental studies about I_h require a low-noise SQUID below 1Hz. I_h controls heartbeat as well as thalamus and hippocampus. Generally calcium ion channel has a very long time constant concerning memory and learning.

It has been believed that rhythmic mode has a good linearity between input and output making contribution to trasfer of sensory information in a awake state to be named transmission mode while burst mode has a poor linearity between input and output only contributing about something in sleep or seisure. However recent experimental data have evidences that burst mode rhythms make contribution to trasfer of sensory information in a awake state. Arousal and serective attention in human brains are controlled by rhythms in both depolarized and hyperpolarized states including focal attention for visual focus.

The whol-head SQUID system of SNS junctions free of telegraph noise in the superconducting magnetic shield has low noise characteristics at low frequencies or long latencies to offer an exellent tool for study on higher function and activites of human brains.

5 Conclusion

We have developed both SQUID of SNS junctions and the superconducting magnetic shield to make the mobile whole-head SQUID system. Research on superconducting weak links including niobium point contact Josephson junctions in the earliest days has finally led us to a brand-new concept of mesoscopic Josephson junction to create a mobile clinic for mental care which would make some contribution to cure of autism, ADHD and depression.

References

1 H. Ohta, M. Aono, T. Matsui, Y. Uchikawa, K. Kobayashi, K. Tanabe, S. Takeuchi, K. Narasaki, S. Tsunematsu, Y. Kamekawa, K. Nakayama, K. Koike, K. Hoshino, H. Kotaka, E. Sudoh, H. Takahara, Y. Yoshida, K. Shinada, M. Takahata, and Y. Yamada, IEEE Trans. on Applied Superconductivity, Vol. 9 (1999) 4073.

2 H. Ohta and T. Matsui Supercond. Sci. Technol. 12, 762 (1999).

3 H. Ohta, A. Koike, K. Hoshino, H. Kotaka, E. Sudoh, K. Kato, H. Takahara, Y. Uchikawa, K. Shinada, M. Takahata, Y. Yamada, and T. Matsui, IEEE Trans. Applied Superconductivity MAG-27 (1993)1953 .

4 H. Ohta and T. Matsui, Y. Uchikawa, K. Kobayashi, and M. Aono, Physica C, Vol. 352, 186, 2001.

5 H. Ohta and T. Matsui, Physics and Applications of Mesoscopic Josephson Junction ed. by H. Ohta and C. Ishii, The Physical Society of Japan, Tokyo Japan, 1999 .

6 J. Vrba, SQUID Sensors : Fundamentals, Fanrication and Applications ed. by H. Weinstock, Kluver Academic Publishers, Tokyo Japan, 1995 .

7 R. R. Llinas, Science, Vol. 242, 1654.

8 X. -J. Wang, Neuroscience, Vol. 59, 1994, 21.

9 J. L. Hindmarsh and R. M. Rose, Phil. Trans. R. Soc. Lond. B (1994) 346, 129; (1994) 346, 151; (1994)

346, 165.
10 E. R. Kandel, J. H. Schwartz, and T. M. Jessell, Principles of Neural Science Fourth edition, McGraw-Hill, 2000.

***OHTA Hiroshi**, Dr. Eng.*

Expert Researcher, Millimeter-Wave Devices Group, Wireless Communications Department

MATSUI Toshiaki

Group Leader, Millimeter-Wave Devices Group, Wireless Communications Department

High Frequency Measurement, Microwave and Millimeter-Wave Devices and Circuits